Allergy and Immunology

AIMS Allergy and Immunology, 5(3): 135–159.
DOI: 10.3934/Allergy.2021011
Received: 26 March 2021
Accepted: 10 May 2021
Published: 14 May 2021

http://www.aimspress.com/journal/Allergy

Research article

Microvesicles produced by monocytes affect the phenotype and functions of endothelial cells

Dmitriy I. Sokolov[1,*], Anastasia R. Kozyreva[1], Kseniia L. Markova[1], Valentina A. Mikhailova[1], Andrey V. Korenevskii[1], Yulia P. Miliutina[1], Olga A. Balabas[2], Sergey V. Chepanov[1] and Sergey A. Selkov[1]

[1] Federal State Budgetary Scientific Institution, Research Institute of Obstetrics, Gynecology, and Reproductology named after D.O. Ott, Saint Petersburg, Russia
[2] Chemical Analysis and Materials Research Centre, Federal State Budgetary Educational Institution of Higher Education, Saint Petersburg State University, Saint Petersburg, Russia

* **Correspondence:** Email: falcojugger@yandex.ru.

Abstract: Monocytes\macrophages regulate angiogenesis via cytokine production and contact interactions with endothelial cells (ECs). The biological effects of macrophage-derived microvesicles (MVs) are studied using cell lines, such as monocytic leukemia THP-1 cell line. The effect of MVs produced by THP-1 cells on EC phenotype and functions remain understudied. In this research, we studied the effect of MVs produced by THP-1 cells on the phenotype, proliferation, migration, and vascular formation of EA.Hy926 ECs. MVs produced by THP-1 cells express CD54, CD18, CD11a, CD11b, CD29, CD120a, CD120b, VEGFR1, VEGFR2, CD105, CD119, TGFR2 on the surface and contain ERK1/2, pERK1/2 Akt, FGF10, endothelin-2. The transfer of an intracellular protein labeled with a fluorescent dye from MVs produced by THP-1 cells to EA.Hy926 ECs was established. It was found that MVs derived from THP-1 cells inhibit EC proliferation. In high concentrations, MVs reduce EC migration, increase the length but decrease the number of vessels formed by ECs, promoting the development of non-branching angiogenesis. On the contrary, in low concentrations, MVs increase EC migration, reduce the length, and increase the number of vessels formed by ECs, promoting the development of branching angiogenesis. Thus, the fundamental possibility of the influence of MVs produced by THP-1 cells on the processes of angiogenesis has been established. Proteins found in the MVs composition may be responsible for the observed effects of MVs on ECs.

Keywords: monocytes; macrophages; endothelium; microvesicles; proliferation; migration; angiogenesis, endoglin; TGFβ; FGF10

Abbreviations: ECs: endothelial cells; MVs: microvesicles; ECM: extracellular matrix; MMPs: metalloproteinases; IQR: interquartile range; CFSE: carboxyfluorescein diacetate succinimidyl ester; MFI: mean fluorescence intensity

1. Introduction

Monocytes\macrophages are actively involved in the angiogenesis regulation [1–3]. They regulate the growth and remodeling of blood and lymphatic vessels in different ways. Macrophages can inhibit angiogenesis by triggering apoptosis in ECs and phagocytizing the resulting cellular detritus. This is characteristic of classically activated macrophages (M1). Alternatively, activated macrophages stimulate angiogenesis by producing angiogenic factors such as VEGF-A, VEGF-C, as well as participating in the selection of the leading cell of the growing vessel [4]. Macrophages are involved in the control of angiogenesis at all stages via the production of cytokines and other substances. They secrete angiogenin and human angiogenic factor (h-AF), which stimulate EC migration [5–7]. Macrophages secrete vasoactive substances such as VEGF and prostaglandins that increase vascular permeability. Macrophages produce VEGF, bFGF, PDGF, IGF, IL-8, IL-6, and FGF10 cytokines that control EC proliferation and migration [6,8]. IFNγ, TNFα, and TGFβ have the opposite effect on the proliferation and migration of ECs [6]. Macrophages are actively involved in both degradation and synthesis of extracellular matrix (ECM) components, which are the most important participant in angiogenesis. Macrophages are the sources for two types of proteases—metalloproteinases (MMPs): MMP2, MMP9 [9], and serine proteases: urokinase-type plasminogen activator (uPA) and its inhibitor (PAI). These enzymes control ECM degradation and release of matrix-related growth factors [10].

Monocytes and macrophages [11], along with many other cells, such as ECs, epithelial cells, nerve cells, tumor cells of various origins, stem cells, cells of the immune system, are producers of MVs. MVs are relatively new objects of biological research, and therefore in the literature, this group of extracellular vesicles is denoted by various terms: shedding vesicles, shedding bodies, ectosomes, MVs [12], and exovesicles [13]. The diameter of MVs varies between studies in the range of 100–1000 nm [14]. They form everywhere on the plasma membrane, budding out into the extracellular space. Proteins and nucleic acids are believed to enter MVs by targeted transport [12,14,15]. Unlike exosomes, the molecular composition of MVs is less well understood, but it is known that depending on the type of producing cells, MVs can be enriched with matrix metalloproteinases [16–18], glycoproteins such as GPIb, GPIIb-IIIa, P-selectin [19–21], and integrins such as Mac-1 [19,22]. The protein profile of MVs is believed to be highly dependent on the type of source cells. It was found that depending on the type of macrophage activation, the characteristics of the produced MVs can vary [23].

The biological effects of macrophage-derived MVs are studied using cell lines, such as THP-1 cell line. The use of cell lines is justified by the fact that it is extremely difficult to isolate MVs derived from a certain cell population from biological fluids. One of the areas of research on MVs composition is the identification of microRNAs in MV fractions obtained from both cell cultures and

peripheral blood. For example, it was shown that MVs derived from monocytic leukemia THP-1 cells contain miRNA-150, and thereby contribute to an increase in the EC transmigration activity. In addition to miRNA-150, the following microRNAs were found in MVs produced by THP-1 cells: miRNA-20a, miRNA-21, miRNA-23a, miRNA-26b, miRNA-27b, miRNA-30d, miRNA-25, miRNA-29d, miRNA-146a, miRNA-181b, miRNA-221, miRNA-320 [24]. The content of some microRNAs in MVs increased, when cells were exposed to LPS, hydrogen peroxide, and oleic/palmitic acids [24,25]. It is believed that microRNAs are selectively packed into MVs, and the vesicular microRNA profile may differ from cellular microRNAs [26]. It was found that MVs derived from THP-1 cells contain Argonaute 2 protein, which is required for microRNA activity [24]. Activation of THP-1 cells with LPS resulted in MV production, which induced expression of adhesion receptors by ECs [27]. Yet, possible influence of MVs derived from unstimulated THP-1 cells on cell phenotype and functions needs to be defined more precisely.

Thus, macrophages are widely represented in the human body and serve as a source of a wide range of biologically active molecules, in particular, cytokines and growth factors, microRNAs. Macrophages are involved in a number of physiological processes, including the regulation of angiogenesis. Monocytes\macrophages produce MVs containing a variety of substances. Currently, the protein component and functions of MVs produced by monocytes\macrophages are poorly understood. In this research, we studied the effect of MVs produced by monocytic leukemia THP-1 cells on the phenotype, proliferation, migration, and vascular formation of EA.Hy926 ECs.

2. Materials and methods

2.1. Cells

THP-1 cell line was obtained from the ATCC (USA). The cell culture was kept in the suspension form at a concentration of 0.7–1 × 10^6 cells/mL in a complete RPMI 1640 medium with 10% fetal calf serum (FCS) (Sigma, USA).

EA.Hy926 ECs were provided by Dr. Edgel (University of North Carolina, NC, USA). The main characteristics of these cells are typical for ECs [28–30]. The cells were cultured as previously reported [31]. Cell viability was checked using Trypan blue solution and comprised an average 96%. All experiments involving cell culturing were performed under the same incubation conditions (humid environment, 37 ℃, 5% CO_2).

2.2. Microvesicle separation

Before the experiments, FCS was frozen while stored and then thawed and inactivated by the standard protocol (heating to 56 ℃). The heating of FCS might lead to the destruction of MVs, which are possibly present in the media. All solutions (including culture media and FCS) for isolating MVs and experimenting on them were filtered through a 0.2 μm pore size filter (Corning, Germany) before the experiments [32]. THP-1 cells were cultured in flasks in DMEM/F-12 supplemented with 10% FCS, 2 mM L-glutamine, 100 U/mL penicillin, and 100 μg/mL streptomycin (Sigma, USA) if else not specified. Further in the article, cells cultured under these conditions are defined as unstimulated. The day before MV separation, the medium was completely replaced with fresh culture medium filtered through a 0.2 μm pore size filter. THP-1 cells were

diluted to a concentration of 1×10^6/mL. Cell viability was assessed the day after culture initiation. We centrifuged the culture media obtained from flasks at 200 g (22 ℃) for 10 min allowing cell removal. Currently, due to the absence of a single standard method for the separation of MVs, various approaches to obtain MV fractions with different purity and enrichment levels are used [33,34]. To separate MVs, we used previously reported differential centrifugation method [35,36]. Briefly, supernatants containing MVs were centrifuged at 500, 9900 and 19800 g. The supernatant was then discarded, and the pellet was resuspended in Hanks' solution without Ca^{2+} and Mg^{2+}.

2.3. Laser correlation analysis

As we previously reported, to control the size of the isolated MVs we used the laser correlation spectrometer (Zetasizer NanoZS, Malvern Instruments, UK) [37]. The experiments were repeated five times. The size of the MVs produced by THP-1 cells was in the range of 169–400 nm (Figure 1).

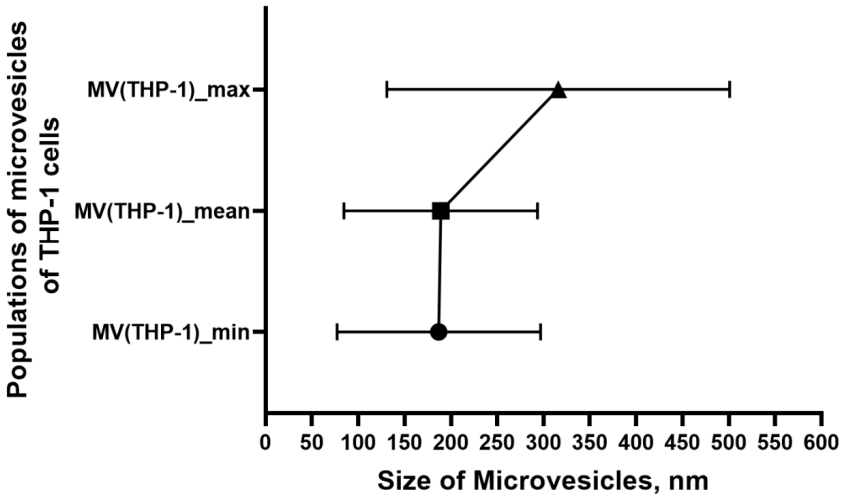

Figure 1. Laser correlation analysis of microvesicles produced by THP-1 cells. MV: microvesicles; MV(THP)_min: minimum size of microvesicles produced by THP-1 cells; MV(THP)_mean: the average size of microvesicles produced by THP-1 cells; MV(THP)_max: maximum size of microvesicles produced by THP-1 cells. Statistical analysis was performed using descriptive statistics.

The peak of the MV quantity distribution was 200 nm. These data complied with previous works [32,36,38,39], which ascertained the size of MVs.

2.4. Analysis of total protein content

The total protein concentration in the cell and MV lysates was determined by the Bradford method [40] using a NanoDrop One spectrophotometer (Thermo Scientific, MA, USA). After culturing for 24 h (as described above), the total protein amount in MVs produced by source THP-1 cells was 0.15 ± 0.036 μg/10^6. The obtained data allowed us to calculate the protein load

of microchips for gel electrophoresis. Based on the total protein amount in MV probes of unstimulated THP-1 cells, we prepared the dilutions of MVs in culture media for further experiments: 3.276 μg/100 μL, 1.638 μg/100 μL, 0.819 μg/100 μL and 0.410 μg/100 μL.

2.5. Phenotypic characteristics of THP-1 cells including MVs

For phenotype evaluation, THP-1 cells were centrifuged for 10 min at 200 g, then cells were diluted to a concentration of 1×10^6 cells per 300 μL of Hanks' solution. MVs isolated from 30 mL of THP-1 cell culture medium were diluted in 1 mL of Hanks' solution containing 0.35% BSA (Sigma, USA). The 100 μL of MV suspension was used for phenotype analysis. THP-1 cells and their MVs were labeled with monoclonal antibodies against CD11a PE-Cy7 clone HI111 (BD, USA), CD11b PerCP clone 238446 (RD, USA), CD11c Alexa Fluor 700 clone ICRF 3.9 (RD, USA), CD18 PE clone 212701 (RD, USA), CD29 PE clone P5D2 (RD, USA), CD54 adhesion molecules FITC clone BBIG-I1 (11C81) (RD, USA); CD119 (IFNγR) FITC clone 92101 (RD, USA), CD120a (TNFαR1) Alexa Fluor 488 clone 16803 (RD, USA), CD120b (TNFαR2) Alexa Fluor 700 clone 22235 (RD, USA), VEGF-R1 PE clone 49560 (RD, USA), VEGF-R2 PerCP clone 89106 (RD, USA), VEGF-R3 APC clone 54733 (RD, USA), TGFβR2 cytokine receptors (RD, USA) Alexa Fluor 700, clone 25508 (RD, USA); HLA-DR phenotypic marker APC-H7 clone L243 (BD, USA) and CD105 APC clone 166707 (RD, USA) according to the manufacturer's instructions. The antibodies were combined into tree panels that we used from MV treatment. Each panel was used to treat 100 μL of MV suspension or 1×10^6 cells in 300 μL of Hanks' solution. The gating strategy used can be found in Figures S1 and S2. The experiments were repeated four times. The receptor expression was assessed using unstimulated THP-1 cells and MVs. Isotype controls (BD and RD, USA) and additionally cells and MVs not treated with antibodies were used. Flow cytometry was conducted using BD FACS Canto II flow cytometer as shown previously [41], which allows detecting particles greater than 0.2 μm in size. To adjust the device, we used additional protocols for cleaning the flowing liquid and sample washing buffers as well as calibration particles of 0.1, 0.2, 0.5 and 1.0 μm (Invitrogen, USA) in size according to the device manufacturer's instructions.

2.6. Evaluation of the effect of MVs derived from THP-1 cells on the proliferative activity of EA.Hy926 ECs

The method was reported previously by us [42]. Briefly, ECs were seeded into 96-well flat-bottom plate. After 24 hours, the medium was replaced with dilutions of MVs derived from unstimulated THP-1 cells prepared using the ECs medium containing 2.5% FCS (3.276 μg/100 μL, 1.638 μg/100 μL, 0.819 μg/100 μL and 0.410 μg/100 μL). After 24 hours, ECs were next stained with 0.2% crystal violet solution as reported previously [43]. Optical density was measured using Microplate Reader (Thermo Labsystems), and converted to the cell number. Changes in cell proliferation were assessed by comparing changes in sample optical density and the cell number with that of the ECs incubated in MV-free culture medium containing 2.5% FCS. When culturing ECs with 10% FCS (positive control), stimulation of ECs proliferative activity (17671 (13637, 34043) cells/well) was observed, compared with ECs culturing in medium with 2.5% FCS (10022 (9990, 10513) cells/well, $p < 0.001$). Experiments were carried out three times with each MV concentration analyzed in four replicates.

2.7. Evaluation of the effect of MVs derived from THP-1 cells on the migration of EA.Hy926 ECs

The method was reported previously by us [42]. Briefly, ECs were cultured for 24 hours in 96-well flat-bottom plate. The monolayer was then disrupted by partial cell scraping, the width of the obtained line was photographed (Figure 2).

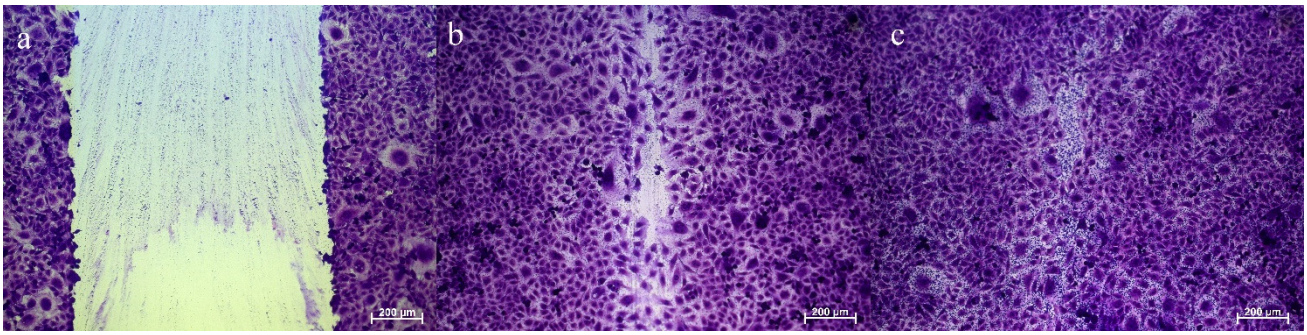

Figure 2. Migration of EA.Hy926 cells. Stained with crystal violet, ×100. (a) Initial width of the disrupted monolayer (migration surface) line. (b) Migration after incubation in medium containing 2.5% FCS for 24 hours. (c) Migration after incubation in medium containing 10% FCS for 24 hours.

Then, the medium was replaced with dilutions of MVs derived from THP-1 cells prepared using the EC medium containing 2.5% FCS (3.276 µg/100 µL, 1.638 µg/100 µL, 0.819 µg/100 µL and 0.410 µg/100 µL). After 24 hours, ECs were incubated with 100 µL of crystal violet solution (0.2%, Sigma-Aldrich Chem. Co., USA), washed and dried. Three fields of view were photographed in each well. Data analysis was performed using MarkMigration (Russia) software [44], which considers the residual area of the disrupted monolayer line after migration. Experiments determining EC migratory activity in the presence of MVs were performed three times. Each MV concentration was analyzed four times. Median area of the initial line after monolayer scraping was 0.88 mm^2 (interquartile range (IQR), 0.88–0.89). No cells in the disrupted monolayer zone were detected. We noted an increase in the number (579 (504, 635), $p < 0.001$) of migrated ECs and a decrease in the area (0.2 (0.14, 0.25), $p < 0.01$) mm^2 of the disrupted monolayer line after cell migration in the presence of 2.5% FCS. An increase in the FCS concentration in cell culture medium to 10% (positive control) caused an increase in the number of migrated ECs (657 (588, 762), $p < 0.01$) and a decrease in the residual area of the disrupted monolayer line after cell migration (0.12 (0.83, 0.18), $p < 0.001$) mm^2. Thus, in the experimental model, EA.Hy926 cells responded to a higher FCS concentration with increased migratory activity, which is consistent with the results described previously [45,46]. This allows the evaluation of changes in cell migratory activity in the presence of MVs derived from THP-1 cells.

2.8. Evaluation of the effect of MVs produced by THP-1 cells on the ability of ECs to form vessels

Wells of a 96-well plate were pretreated with the Matrigel Growth Factors Reduced matrix (BD, USA) as we reported earlier [47]. Matrigel is a mixture of extracellular matrix proteins, and also contains minor levels of cytokines (TGFβ, EGF, IGF, bFGF, and PA) [48]. Then, EA.Hy926 ECs

were added to the wells (150000 cells/mL in 200 μL of culture medium). MVs derived from THP-1 cells at different concentrations in 100 μL of culture medium were added to some of the wells (3.276 μg/100 μL, 1.638 μg/100 μL, 0.819 μg/100 μL and 0.410 μg/100 μL). The ECs culturing with 2.5% FCS determined baseline parameters. For use as positive controls, ECs were cultured with 20 ng/mL bFGF (RD, USA) or with 10% FCS that was free of MVs. The cells were then incubated for 24 hours. The experiments were performed four times with three replicates for each MV concentration. Data were recorded in all experiments using the AxioObserver.Z1 microscope (Zeiss, Germany) and the Axiovision image analysis software (Zeiss, Germany). In each well, one field of view was taken into consideration, in which length (in micrometers (μm)) and number of vessels were estimated using the ImagePro software.

2.9. Evaluation of the fluorescent tag transfer from MVs derived from THP-1 cells to EA.Hy926 ECs

We used the method described earlier [42]. Briefly, ECs were seeded into a 96-well plate (3.5×10^4 cells/well in 100 μL of medium) and cultured for 24 hours. To stain intracellular protein, THP-1 cells were treated with a carboxyfluorescein diacetate succinimidyl ester (CFSE, Sigma, USA) solution at concentration of 5 μM (n = 5) for use as positive controls. Some THP-1 cells were left unstimulated. Unstimulated and stained THP-1 cells were then cultured in 75 cm^2 flasks (BD, USA) in 40 mL of complete RPMI1640 for 24 hours. The cell concentration was 1×10^6/mL. MVs were then isolated (as described above), added to ECs (3.276 μg of total protein in 100 μL of medium), and incubated for 24 hours. ECs were washed three times with Versene solution and removed from the plate surface. Then, ECs were resuspended twice in Hanks' solution without Ca^{2+} and Mg^{2+}, and centrifuged at 200 g for 10 min. Fluorescent CFSE inclusions in ECs were evaluated using the FACS Canto II flow cytometer (Becton Dickinson, USA). The experiments were repeated five times.

2.10. Evaluation of the effect of MVs derived from THP-1 cells on the phenotype of EA.Hy926 ECs

The detailed method was described earlier [42]. Briefly, MVs derived from THP-1 cells were added to ECs at a total protein concentration of 3.276 μg in 100 μL of medium (in three repetitions). Unstimulated ECs were used as controls. ECs incubated with phorbol 12-myristate 13-acetate (10 ng/mL, Sigma, USA) were used as positive controls. The next day, ECs were washed, removed from the plate with Versene solution and stained with 7-AAD dye (Biolegend, USA). Cell death was assessed using the BD FACS Canto II flow cytometer by 7-AAD inclusion, as described [49,50]. The median pool of nonviable ECs after culturing with MVs derived from THP-1 cells was 8.9% (IQR 4.5–9.5). Viability experiments were repeated four times. After incubation with MVs, ECs were treated with monoclonal antibodies against CD45 PerCP clone 2D1, CD54 APC clone HA58, CD29 PE clone MAR4, CD11a FITC clone HI111, CD11b PE clone ICRF44, and CD18 APC clone 6.7 (Becton Dickinson, USA), as well as with isotypic antibodies. Antibody selection was based on phenotyping results of THP-1 cells and their MVs. The fluorescence was analysed using the BD FACS Canto II cytometer. Analysis of the receptor expression in ECs was repeated four times.

2.11. Western blot analysis

Unstimulated THP-1 cells and their MVs were washed with cooled phosphate buffer (0.01 M PBS, pH 7.4) and then lysed in RIPA buffer 50 mM Tris-HCl, pH 8.1, Triton X-100 (1%), sodium deoxycholate (0.5%), sodium dodecyl sulfate (0.1%), sodium chloride (150 mM), and ethylenediaminetetraacetic acid (EDTA) (1 mM) containing a protease and phosphatase inhibitor mixture (Sigma, USA) with intermittent shaking for 30 min. Cell debris was removed by centrifugation (16000 g, 4 ℃, 10 min). Proteins were normalized for cells and their MVs by 20 μg total protein per assay. Then they were separated by their molecular weight as we previously reported [42]. The proteins were then incubated with primary monoclonal antibodies to Erk1/2 (p44/42 MAPK (Erk1/2), rabbit Ab, 1:1000, Cell Signaling, MA, USA), Phospho-Erk1/2 (phospho-p44/42 MAPK) ((Thr202/Tyr204) (20G11), rabbit Ab, 1:1000, Cell Signaling, USA), Akt (Akt (pan)), (C67E7), rabbit Ab, 1:1000, Cell Signaling, MA, USA), Phospho-Akt ((Ser473) (193H12), rabbit Ab, 1:1000, Cell Signaling, MA, USA) or TGF-β (TGF-beta rabbit Ab 1:1000, Cell Signaling, MA, USA) at 4 ℃ for one night on MR-12 Rocker-Shaker (BioSan, Latvia). After reaction with an appropriate secondary antibody (1:1000; Cell Signaling Technology, MA, USA), signals were visualised on ChemiDoc™ Touch Gel Imaging System (Bio-Rad Laboratories, USA) using enhanced chemiluminescence (ECL) with ECL reagents (Bio-Rad Laboratories, USA). The results were evaluated using ImageLab software (Bio-Rad Laboratories, USA). Based on existing recommendations [51], the intensity of the bands of investigated proteins detected by the Western blotting was normalized by the total protein content in the sample, which was recorded with a gel using stain-free technology (Bio-Rad Laboratories, USA). Samples of three independent experiments (n = 3) were analysed to determine each protein.

2.12. Evaluation of protein profiles of THP-1 cell lysates and their MVs

The procedure was conducted as previously reported [42]. Briefly, the sediments containing cells and MVs were stored at –80 ℃ until assay. The cell membranes were disrupted with five freeze-thaw cycles and mechanical disruption, and the obtained lysates were then centrifuged (16000 g, 4 ℃, 10 min). The obtained supernatants were discarded, and the sediment was dried at room temperature. Next, the dry residue was dissolved in a minimal amount of 0.1 M sodium bicarbonate (Sigma). After determining the total protein amount (as described in Section 2.4), the concentrations of obtained protein solutions were aligned, focusing on the lowest value of the measured protein amount. Purified proteins in obtained solutions were then separated in Agilent 2100 bioanalyzer (Agilent Technologies, USA). All experiments were repeated six times independently.

2.13. One-dimensional gel electrophoresis and trypsinolysis of THP-1-derived MV lysate

MV proteins were fractionated in a 10% polyacrylamide gel under Laemmli denaturing conditions at a load of 42 μg total protein. After electrophoretic separation of proteins, they were visualized by Coomassie G250 staining, then the bands on a gel corresponding to the protein bands were cut out in a number of 35 pieces. Next, the strips were crushed and washed three times to remove the dye and sodium dodecyl sulfate with a solution of 50% acetonitrile in 30 mM Tris (pH 8.2) for 15 min at room temperature. After removing the solution, the gel pieces washed

from the dye were dehydrated in 100% acetonitrile. Then, after removing acetonitrile, the samples were dried for 40 min at 4 ℃. Bovine trypsin solution (20 ng/mL; Promega, United States) was added to the dried samples and incubated for 1 hour on ice until the gel was completely rehydrated. After that, the excess trypsin was removed. 50 μL of 30 mM Tris (pH 8.2) were added to the samples and incubated for 16–18 hours at 37 ℃. Tryptic peptide mixture was extracted three times from the gel with a 50% aqueous acetonitrile solution containing 0.1% formic acid (Sigma-Aldrich Chem. Co., USA) in an ultrasonic bath for 20 min. The peptides in the resulting solution were dried at 4 ℃ and frozen at −80 ℃ until further analysis.

2.14. MALDI-TOF mass spectrometry analysis of tryptic peptide mixtures

After one-dimensional gel electrophoresis and subsequent sample preparation, the dried tryptic peptides were dissolved in 50 μL of a 50% aqueous solution of acetonitrile containing 0.1% trifluoroacetic acid (Sigma-Aldrich Chem. Co., USA), and stirred until complete dissolution. The solutions were applied to metal plates for MALDI-TOF mass spectrometry analysis as we previously reported [42]. Mass spectra of the tryptic peptides were obtained using the Axima Resonance MALDI-TOF mass spectrometer (Shimadzu/Kratos Analytical Ltd., UK). Protein identification was undertaken relative to the SwissProt and NCBI databases using taxonomic constraints for the *Homo sapiens* species, the Mascot software (www.matrixscience.com) and the peptide fingerprinting method. A parallel search was performed using a database of inverted and random (decoy) amino acid sequences. After peptide identification, the correspondence between an identified protein and its actual position on a gel was checked.

Statistical analysis was performed in Statistica 10 software. We used the nonparametric Mann–Whitney U test. Data were presented as a median (upper quartile, lower quartile). Results of western blot analysis and enzyme activity assessment were presented as a mean ± standard error of the mean (SEM) within at least three independent experiments. T-test for independent samples was used to analyze the experimental results. The value $p < 0.05$ was considered statistically significant.

3. Results

3.1. Phenotypic characteristics of THP-1 cells including MV

We found that THP-1 cells carry on their surface CD54 [52,53], CD18 [53], CD11b [52], CD11a [53,54], CD29 adhesion molecules, CD120a (TNFαR1) [55], CD120b (TNFαR2) [56], VEGFR1 [57], CD105 [58], CD119 (IFNγR1) [59], TGFR2 [60] cytokine receptors, HLA-DRA [61] major histocompatibility complex (Figure 3). Expression of VEGF-R2 [57], CD11c [62], and VEGF-R3 [63] by THP-1 cells was very low. Our findings are consistent with published data (references are indicated above next to each receptor). Analysis of the expression of cell surface molecules on MVs produced by THP-1 cells showed that they expressed CD54, CD18, CD11a (Figure 3), CD11b, CD29 adhesion molecules, CD120a, VEGFR1, VEGFR2, CD105, CD119, TGFR2 cytokine receptors, as well as HLA-DR molecule.

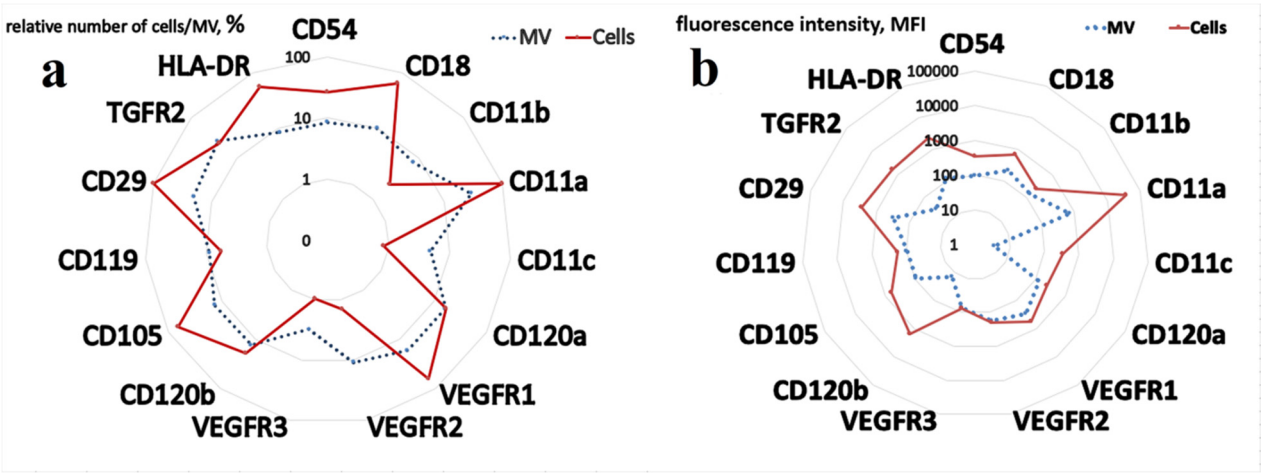

Figure 3. Comparison of phenotypic profiles of THP-1 cells and their MVs. (a) relative number; (b) mean fluorescence intensity (MFI) of the studied markers. Statistical analysis was performed using the non-parametric Mann–Whitney U test.

3.2. Evaluation of the fluorescent tag transfer from MVs derived from THP-1 cells to EA.Hy926 ECs

We established that EA.Hy926 ECs that were incubated with MVs derived from THP-1 cells and pretreated with CFSE solution, included fluorescent CFSE (Figure 4).

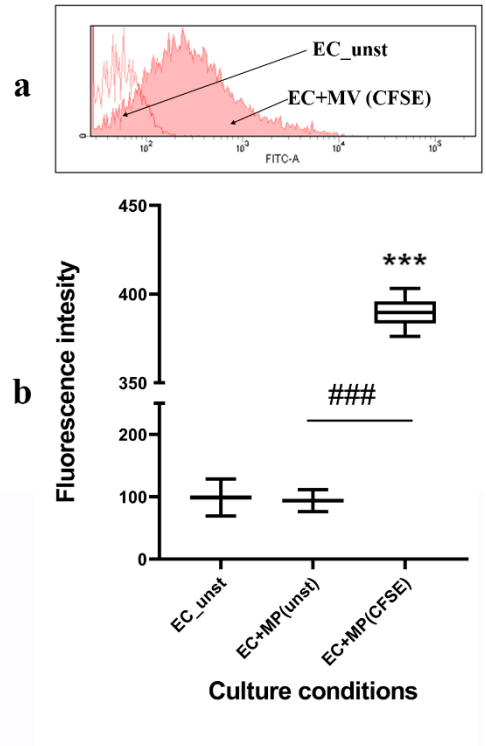

Figure 4. Changes in the fluorescence intensity of ECs after culturing with MVs derived from THP-1 cells stained with CFSE: (a) fluorescence intensity plot, (b) box plot of CFSE MFI. EC_unst: fluorescence of unstimulated ECs; EC + MV (unst): fluorescence

of ECs after incubation with MVs derived from unstimulated THP-1 cells; EC + MV (CFSE): fluorescence of ECs after incubation with MVs derived from THP-1 cells stained with CFSE. Statistical significance: ***p < 0.001—difference compared with the autofluorescence level; ###p < 0.001—difference compared with the fluorescence level of cells cultured with MVs derived from unstained THP-1 cells. Statistical analysis was performed using the non-parametric Mann–Whitney U test. Data were presented as a median (upper quartile, lower quartile).

3.3. Effect of MVs derived from THP-1 cells on the phenotype of EA.Hy926 ECs

Culturing of ECs with MVs derived from THP-1 cells did not affect the constitutive expression of CD29 and CD54 (Figure 5). After ECs culturing with MVs derived from THP-1 cells, CD45, CD11a, CD11b, and CD18 receptors were not transferred to ECs.

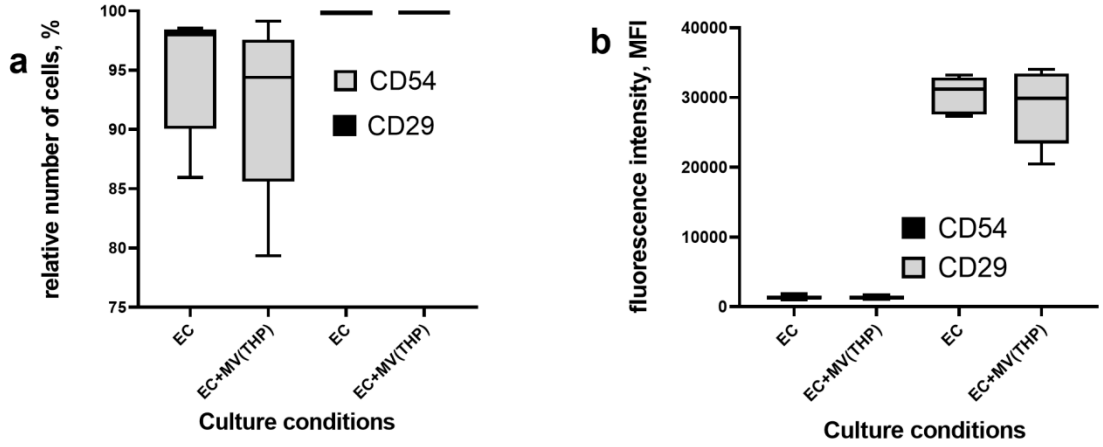

Figure 5. Expression of Receptors by ECs after Culturing with (EC + MV (THP-1)) and without (EC) MVs Derived from THP-1 Cells: (a) relative number of cells, (b) MFI of CD54 and CD29. Statistical analysis was performed using the nonparametric Mann-Whitney U test. Data were presented as a median (upper quartile, lower quartile).

3.4. Proliferative activity of EA.Hy926 ECs in the presence of MVs produced by THP-1 cells

Culturing of ECs with MVs with a total protein content of 3.276 μg/100 μL, 1.368 μg/100 μL, and 0.819 μg/100 μL showed a decrease in EC proliferation compared with EC culturing in a medium without MVs (Figure 6).

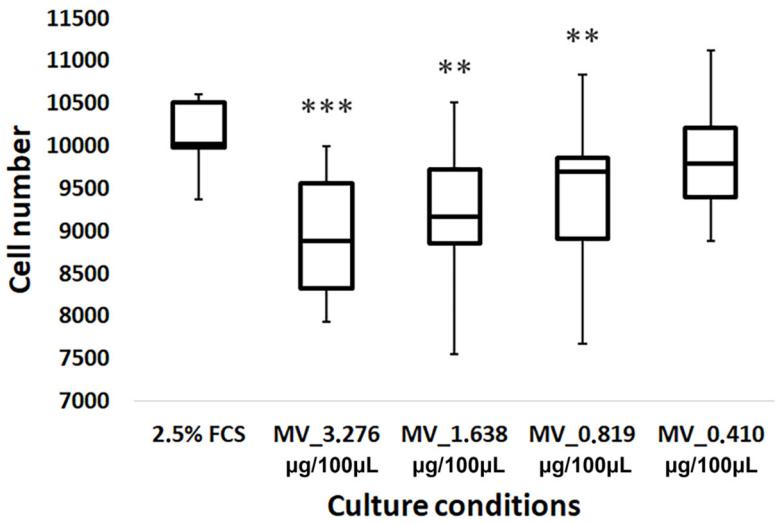

Figure 6. Effect of MVs derived from THP-1 cells on the proliferation of EA.Hy926 ECs. **p < 0.01; ***p < 0.001—difference compared with cells incubated without MVs (2.5% FCS). Statistical analysis was performed using the non-parametric Mann–Whitney U test. Data were presented as a median (upper quartile, lower quartile).

3.5. Migratory activity of EA.Hy926 ECs in the presence of MVs produced by THP-1 cells

ECs cultured with MVs derived from THP-1 cells (total protein content 3.276 µg/100 µL) decreased the migratory activity due to a lower number of migrated ECs compared with ECs cultured without MVs (Figure 7). ECs cultured with MVs derived from THP-1 cells (total protein content 3.276 µg/100 µL and 0.410 µg/100 µL) increased the migratory activity due to an increased number of migrated ECs and in parallel due to a decreased residual area after cell migration to the disrupted monolayer zone (Figure 7).

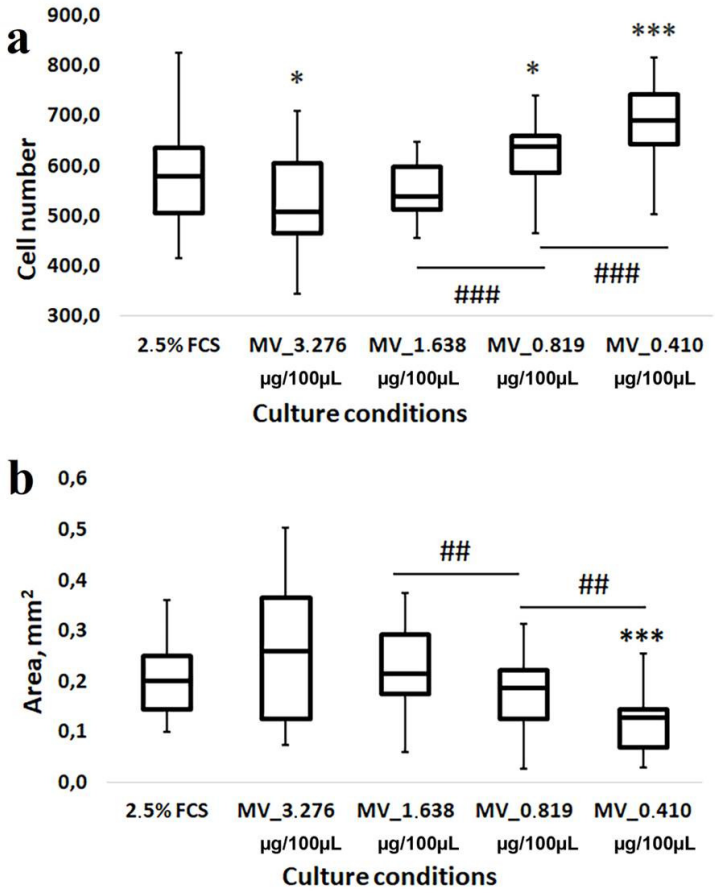

Figure 7. Effect of MVs derived from THP-1 cells on the migratory activity of EA.Hy926 ECs. (a) number of cells that migrated to the disrupted monolayer zone; (b) residual area after migration of cells to the disrupted monolayer zone. ***$p < 0.001$—difference compared with cells incubated without MVs (2.5% FCS); ###$p < 0.001$, ##$p < 0.01$—difference compared with a lower concentration under the same conditions. Statistical analysis was performed using the nonparametric Mann–Whitney U test. Data were presented as a median (upper quartile, lower quartile).

3.6. Vascular formation of EA.Hy926 ECs in the presence of MVs produced by THP-1 cells

In the presence of bFGF, as well as in the presence of 10% FCS, the length of vessels was greater compared to ECs culturing with 2.5% FCS. Culturing of ECs with bFGF lowered the number of vessels, compared to ECs culturing with 2.5% FCS, while culturing in a medium supplemented with 10% FCS did not change their number (Figures 8 and 9). MVs derived from THP-1 cells, at a concentration of 3.276 μg per 100 μL increased the length, and at a concentration of 1.638 μg per 100 μL, on the contrary, decreased the length of vessels, as compared with ECs culturing with 2.5% FCS. The length of vessels formed by ECs in the presence of MVs at a concentration of 1.638 μg per 100 μL was also shorter compared to the length in the presence of MVs at a concentration of 3.276 μg per 100 μL. The number of vessels in the presence of MVs at a concentration of 3.276 μg per 100 μL was lower, and in the presence of MVs at a concentration of 1.638 μg per 100 μL was higher compared to ECs culturing with 2.5% FCS.

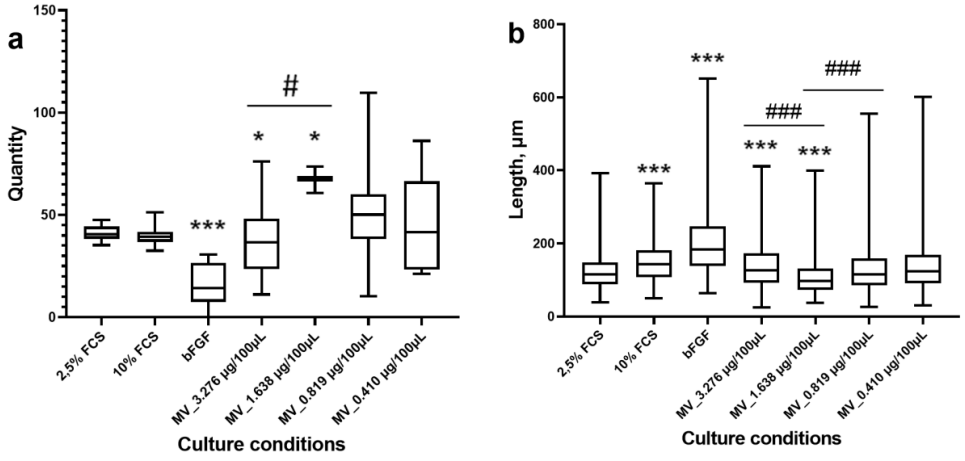

Figure 8. Effect of MVs derived from THP-1 cells on the formation of vessels by EA.Hy926 ECs: (a) the quantity of vessels, (b) the length of vessels. **p < 0.05, ***p < 0.001—difference compared with cells incubated without MVs (2.5% FCS); #p < 0.05, ###p < 0.001—difference compared with a lower concentration under the same conditions. Statistical analysis was performed using the non-parametric Mann–Whitney U test. Data were presented as a median (upper quartile, lower quartile). The length was measured in micrometers (µm).

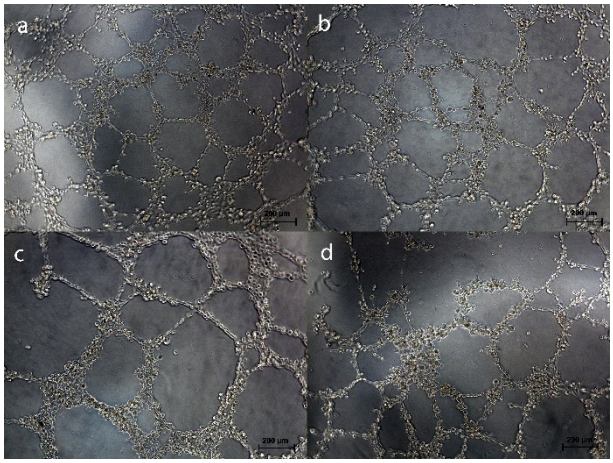

Figure 9. Microscopic photos of vessels formed by ECs under different conditions. (a) in the presence of 2.5% FCS (baseline); (b) in the presence of 20 ng/ml FGF; (c) in the presence of 10% FCS; (d) in the presence of MVs derived from THP-1 cells (0.410 µg of total protein in 100 µL of medium). Phase contrast, ×100.

3.7. Evaluation of protein profiles of THP-1 cell lysates and their MVs

Protein extraction from lysates with microelectrophoresis revealed that 17 and 5 major (>3% of the total intensity) protein groups were released in THP-1 cells and in their MVs, respectively (Figure 10, Table 1). The group with a mean molecular weight of 60.5 ± 0.27 kDa is common for

cells (4.4 ± 0.46%) and their MVs (62.0 ± 2.85%). The groups with the following masses also predominated in cells: 42.7 ± 0.28 kDa (22.6 ± 2.25%); 12.8 ± 0.09 kDa (11.3 ± 1.41%); 11.9 ± 0.04 kDa (7.2 ± 0.85%); 28.4 ± 0.19 kDa (6.6 ± 0.27%) and 66.6 ± 0.45 kDa (6.8 ± 0.62%). Protein groups with masses of 98.0±1.03 kDa (12.1 ± 0.87%) and 84.7 ± 0.17 kDa (6.9 ± 0.44%) predominated in MVs. Thus, protein profiles of THP-1 cells and their MVs differed: cells contained a greater variety of proteins than MVs did, while proteins with a higher molecular weight predominated in MVs compared to that in THP-1 cells.

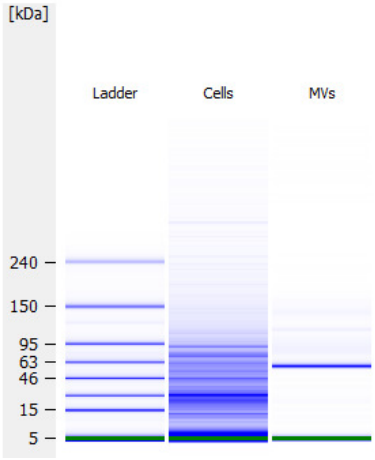

Figure 10. Electrophoregrams of THP-1 cell lysates and their MVs.

Table 1. Major components of the protein profile of THP-1 cells and their MVs (M ± m, n = 5–6; 700 μg of total protein amount per ml of lysate).

	No.	Molecular weight, kDa	Pool, %
Cells, n = 6	1	11.2 ± 0.05	4.1 ± 0.31
	2	11.9 ± 0.04	7.2 ± 0.85
	3	12.8 ± 0.09	11.3 ± 1.41
	4	14.5 ± 0.06	5.6 ± 0.36
	5	18.1 ± 0.01	5.0 ± 0.46
	6	20.1 ± 0.07	3.9 ± 0.18
	7	23.0 ± 0.18	3.5 ± 0.23
	8	24.9 ± 0.14	4.2 ± 0.53
	9	28.4 ± 0.19	6.6 ± 0.27
	10	34.4 ± 0.20	5.6 ± 0.67
	11	42.7 ± 0.28	22.6 ± 2.25
	12	50.7 ± 0.27	3.6 ± 0.18
	13	54.7 ± 0.07	5.1 ± 0.77
	14	57.0 ± 0.35	4.5 ± 1.74
	15	59.9 ± 0.33	4.4 ± 0.46
	16	66.6 ± 0.45	6.8 ± 0.62
	17	83.2 ± 0.31	3.6 ± 0.46
MVs, n = 5	1	61.1 ± 0.45	62.0 ± 2.85
	2	84.7 ± 0.17	6.9 ± 0.44
	3	98.0 ± 1.03	12.1 ± 0.87
	4	120.7 ± 0.67	5.8 ± 2.02
	5	138.2 ± 0.68	6.6 ± 1.83

3.8. MALDI-TOF mass spectrometry analysis

It was shown that apart from other proteins identified, MVs derived from THP-1 cells presumably contained fibroblast growth factor (fibroblast growth factor 10, encoded by the FGF10 gene; SwissProt entry O15520, MW 23.4 kDa, pI 9.61, 7 tryptic peptides, overlapping 9% of the amino acid sequence of the protein) and endothelin precursor (endothelin-2 isoform 2 preproprotein, encoded by the EDN2 gene; NCBI entry NP_001289198, MW 16.5 kDa, pI 10.19, 7 tryptic peptides, overlapping 11% of the amino acid sequence of the protein). These two proteins were recognized as associated with angiogenesis. The other proteins identified included cytoskeleton proteins, protein biosynthesis enzymes, energy metabolism enzymes, etc.

3.9. Western blot analysis

THP-1 cells and their MVs contained ERK1/2, Akt, and TGFβ. Regarding the total protein in MVs and THP-1 cells, respectively, the total ERK1/2 kinase content in MB was 6.4 times less than its content in THP-1 cells. However, it was shown that a significant amount of phosphorylated form of ERK1/2 (pERK1/2) was present in MVs produced by THP-1 cells, compared to THP-1 cells. It was shown that MVs contained protein kinase Akt in the amount comparable to that in THP-1 cells, while there were no endogenous levels of Akt phosphorylated by Ser473 revealed (Figure 11).

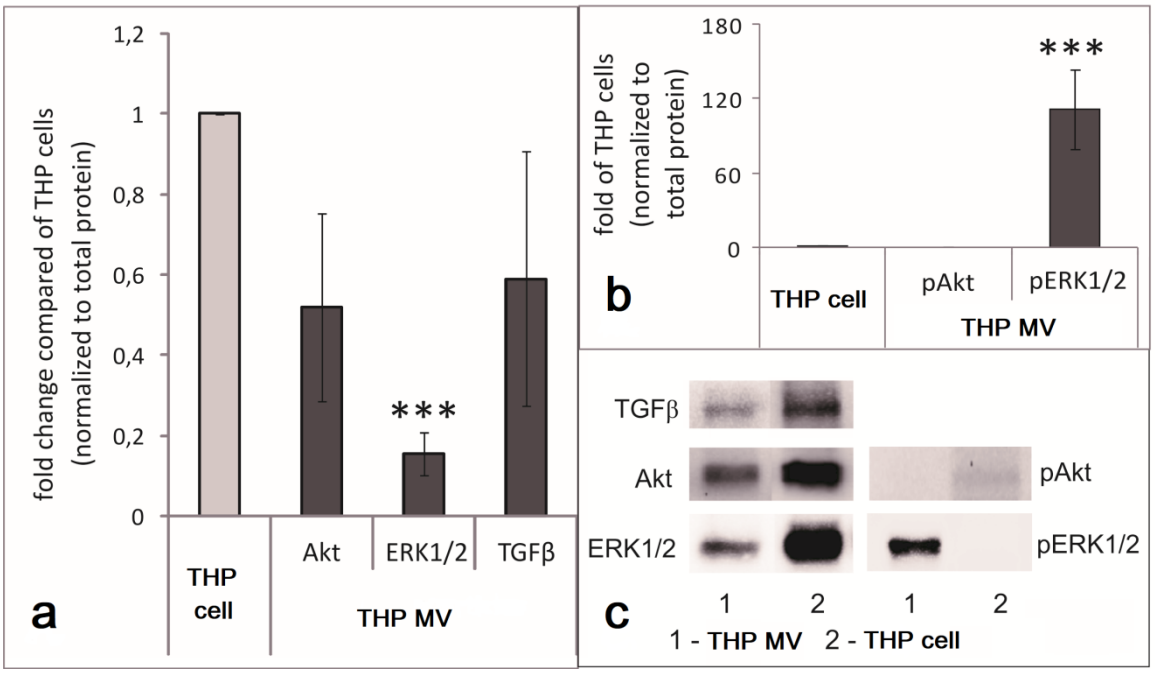

Figure 11. Comparative analysis of protein content in THP-1 cells and their MVs by immunoblotting. (a) content of ERK1/2, Akt and TGFβ in THP-1 cells and their MVs. (b) content of phosphorylated forms of ERK1/2 (pERK1/2) and Akt (pAkt) kinases in THP-1 cells and their MVs. Western blot data were normalized by the total protein, and the content of the investigated proteins in MVs was calculated in relation to their content in THP-1 cells (n = 3). (c) representative immunoblots showing the content of common

Erk1/2 and Akt kinases and their phosphorylated forms (pERK1/2 and pAkt), as well as latent TGFβ in lysates (20 μg) of THP-1 cells and their MVs. THP MVs-1, THP cells-2. ***$p < 0.001$—difference between the protein content in MVs and its content in THP-1 cells. Statistical analysis was performed using the parametric T-test. Data were presented as a mean ± standard error of the mean (SEM).

4. Discussion

The interaction of monocytes\macrophages with ECs determines the course of many biological processes, such as inflammation, angiogenesis, carcinogenesis, atherogenesis [64–67]. The possibility of interaction of these cells using MVs is of particular interest. Therefore, we attempted to describe this interaction. Monocytic leukemia THP-1 cells were selected as source cells of MVs, and EA.Hy926 ECs were selected as target cells.

Comparison of the phenotype of monocyte leukemia THP-1 cells and their MVs indicated a coincidence of profiles of the molecules they express (Figure 3). The presence of CD54, CD18, CD11a, CD11b, and CD29 adhesion receptors on the MVs surface may determine their further interaction with target cells [68–70].

Due to the expression of ligands for these molecules [71], ECs can be targets for MVs derived from monocytes/macrophages. The presence of CD120a (TNFαR1), CD120b (TNFαR2), VEGFR1, VEGFR2, CD105, CD119 (IFNγR1), TGFR2 receptors on MVs derived from THP-1 cells can be a trap for the corresponding cytokines similar to soluble receptors capable of binding cytokines and canceling their effect on target cells [72]. On the other hand, being part of MV membrane, these receptors may be shed from monocytes/macrophages, thus decreasing the sensitivity of cells to the corresponding cytokines.

Currently, there are literature data describing several potential ways for MVs to interact with target cells: simple membrane fusion, clathrin- and caveolae-mediated endocytosis, lipid raft-dependent endocytosis, phagocytosis, micropinocytosis, destruction of MVs near target cells followed by the effect of the contents on target cells via surface receptors [12,73–75]. The pathway of MVs internalization in target cells depends largely on which proteins and glycoproteins are expressed both on MVs themselves and on recipient cells [76]. We established the transfer of an intracellular protein labeled with a fluorescent dye from MVs produced by THP-1 cells to EA.Hy926 ECs (Figure 4). This coincides with previously obtained data on the protein transfer by MVs derived from natural killer cells to ECs [42]. Despite this, we were not able to detect the transfer of CD45, CD11a, CD11b, and CD18 receptors to the endothelium by MVs derived from THP-1 cells. In a similar model, the transfer of CD45 receptors by MVs derived from natural killer cells to ECs was previously established [42]. In the case of MVs produced by THP-1 cells, the absence of transfer of surface receptors to the endothelium can be explained by their low concentration on the MVs membrane or by differences in the uptake mechanisms of MVs derived from monocytes\macrophages and natural killer cells by ECs, which requires additional study. Surface receptor transfer from MVs towards target cells can also be influenced by presence or absence of activation triggers for MV source cells. For example, THP-1 cells cultured in the presence of LPS produced MVs, which influenced adhesion receptor expression by ECs [27]. The amount of CD54+ MVs obtained from LPS-stimulated monocytes differed from MVs of unstimulated cells [77].

Further experiments are needed to explore the impact of inducers on MV receptor transfer to recipient cells.

We established the fundamental possibility of the influence of MVs produced by THP-1 cells on the processes of angiogenesis. Thus, MV derived from THP-1 cells inhibited ECs proliferation. In high concentrations, MVs reduced ECs migration, increased the length but decreased the number of vessels, promoting the development of non-branching angiogenesis. On the contrary, in low concentrations, MVs increased ECs migration, reduced the length, and increased the number of vessels, promoting the development of branching angiogenesis. This opposite effect of different MV concentrations on the type of angiogenesis may be associated with several factors. On the one hand, an increased number of MVs with VEGFR1 and VEGFR2 receptors may promote binding of VEGF [78] from the medium, which is produced by ECs themselves [79]. A decreased concentration of free VEGF can help reduce the vascular branching [80,81]. An increased content of MVs carrying CD105 on their surface can affect ECs in the same way as the secretory form of this receptor, sCD105 (Endoglin), does. In the literature, we found no data on the difference in effects of these forms of CD105 on ECs.

However, Endoglin was found to dose-dependently inhibit EC migration and the branching pathway of angiogenesis [82]. Using Western Blot Analysis, we established the presence of TGFβ in MVs produced by THP-1 cells. With an increased MV content, the probability of TGFβ destruction near target cells also increased. In our model, this may contribute to a local increase in the TGFβ content near ECs. Previously, TGFβ was found to inhibit EC proliferation and migration [83], promote vascular stabilization, inhibit vascular branching in the absence of VEGF [84], and suppress FGF signaling in ECs. On the other hand, in our model, a decreased number of MVs derived from THP-1 cells may reduce VEGF binding, reduce the effect of Endoglin and change the effect of TGFβ on ECs, and bring to the fore the effect of substances contained in MVs.

Comparison of proteomic profiles of THP-1 cells and their MVs showed a significant difference in their proteomic profiles. Using Western Blot Analysis, we established the presence of ERK1/2 and its phosphorylated form (pERK1/2), unphosphorylated Akt, in MVs produced by THP-1 cells. Using MALDI-TOF mass spectrometry, we found that MVs derived from THP-1 cells contained fibroblast growth factor 10 (FGF10) and endothelin precursor (ET)-2 (endothelin-2 isoform 2 preprotein).

Endothelin-2 found in MVs produced by THP-1 cells, as well as ET-1, acted on ECs via ET_A and ET_B receptors [85]. Activation of these receptors stimulated endothelium NO synthase-mediated NO production by ECs as well as prostacyclin synthesis [86]. ET-1 has been shown to directly promote tumor angiogenesis by inducing EC survival, proliferation, and invasion in an ET_BR-dependent manner [87]. In this context, monocytes\macrophages, due to the production of MVs with ET, can act as regulators of physiological and pathological angiogenesis [87].

Previously, FGF10 was found to enhance the stimulating effect of VEGF on EC proliferation [88]. In lung development, FGF10 enhances airway branching via ERK1/2 and mTORC1 [89]. The receptors for FGF10 are FGFR1b and FGFR2b [90], which are expressed on ECs [91,92]. It is possible that FGF10 is able [93] to stimulate branching angiogenesis by acting on ECs via these receptors in the same way as bFGF [94]. Despite the fact that FGF10 and bFGF can affect ECs via the same receptors, no direct evidence has been found in the literature in favor of the effect of FGF10 on branching angiogenesis. FGF signals through the RAS-MAPK and PI3K-AKT-GSK3β signaling pathways. FGF10 signaling through FGFR2b to SRC induce F-actin binding protein phosphorylation as well as cortactin phosphorylation, which participates in

endocytosis and clathrin-dependent internalization [95]. FGF10 signaling stimulates the polarization of FGFR2b to the leading edge for the regulation of cellular migration [95]. A triple membrane signaling pathway has been described, in which stimulation of FGFR2b or VEGFR2 receptor tyrosine kinases activates ADAM17 followed by HB-EGF release, EGFR activation, and ERK1/2 activation. The result of this signal is stimulation of EC migration [91]. Thus, the observed effects of migration, stimulation, and activation of branching angiogenesis in the presence of small numbers of MVs may be the result of a predominant effect of FGF10 and pERK1/2 localized in MVs on ECs. Despite the presence of TGFβ in MVs and its ability to inhibit branching angiogenesis in the absence of VEGF [84], its ability to stimulate this type of angiogenesis has been established in certain cases. It was found that TGFβ stimulated vascular branching in the conditioned medium of glial cells [96]. Low extracellular TGFβ levels also promote EC proliferation and migration and new blood vessel formation [84]. High TGFβ concentrations induce EC differentiation, tube formation reduction, and impaired invasion in artificial matrix. Previously it was shown that TGFβ similarly to VEGF is able to induce angiogenesis and that VEGF can be a target for TGFβ [84]. TGFβ is known to crosstalk between different signaling pathways and to promote expression of other factors that affect angiogenesis, e.g., VEGF [97], FGF [98]. In this context, a decrease in the concentration of MVs in the EC microenvironment may lead to a decrease in the release of TGFβ, which, under conditions of a decreased VEGF deprivation by VEGFR receptors on MVs and in the presence of FGF10, may stimulate branching angiogenesis.

5. Conclusions

Thus, MVs derived from monocytes\macrophages have the ability to regulate angiogenesis, i.e., affect proliferation, migration, determine the method of vascular formation, and stimulate branching or non-branching angiogenesis. MVs produced by THP-1 cells are able to interact with ECs and transfer protein into them due to the receptor expression on the membrane. CD105, TGFβ, pERK1/2, FGF10, and preproprotein endothelin-2, which are potentially capable of changing the behavior of ECs in the manner we discovered, and correcting angiogenesis, were found in the composition of MVs derived from THP-1 cells.

Conflict of interest

All authors declare no conflicts of interest in this paper.

Acknowledgements

The authors thank V.A. Semyonov for assistance in managing cell cultures. The study was supported by AAAA-A19-119021290116-1 (cell line culturing). Phenotyping of THP-1 cells and their MVs, assessment of proliferation, migration, and vascular tube formation, WesternBlot and MALDI-TOF-mass spectrometry analysis was supported by RFBR grant No. 19-015-00218. Participation of A.R. Kozyreva was supported by the scholarship of the President of the Russian Federation SP-420.2019.4. The funders did not participate in the design, data collection or analysis of this research, or preparation or publication of this manuscript. Mass spectrometry analysis was performed in the Chemical Analysis and Materials Research Centre of the Federal State Budgetary

Educational Institution of Higher Education: Saint Petersburg State University, Saint Petersburg, Russia.

References

1. Bingle L, Lewis CE, Corke KP, et al. (2006) Macrophages promote angiogenesis in human breast tumour spheroids in vivo. *Brit J Cancer* 94: 101–107.
2. Riabov V, Gudima A, Wang N, et al. (2014) Role of tumor associated macrophages in tumor angiogenesis and lymphangiogenesis. *Front Physiol* 5: 75.
3. Fantin A, Vieira JM, Gestri G, et al. (2010) Tissue macrophages act as cellular chaperones for vascular anastomosis downstream of VEGF-mediated endothelial tip cell induction. *Blood* 116: 829–840.
4. Schmidt T, Carmeliet P (2010) Blood-vessel formation: Bridges that guide and unite. *Nature* 465: 697–699.
5. Olivo M, Bhardwaj R, Schulze-Osthoff K, et al. (1992) A comparative study on the effects of tumor necrosis factor-alpha (TNF-alpha), human angiogenic factor (h-AF) and basic fibroblast growth factor (bFGF) on the chorioallantoic membrane of the chick embryo. *Anat Rec* 234: 105–115.
6. Sunderkotter C, Goebeler M, Schulze-Osthoff K, et al. (1991) Macrophage-derived angiogenesis factors. *Pharmacol Therapeut* 51: 195–216.
7. Hockel M, Sasse J, Wissler JH (1987) Purified monocyte-derived angiogenic substance (angiotropin) stimulates migration, phenotypic changes, and "tube formation" but not proliferation of capillary endothelial cells in vitro. *J Cell Physiol* 133: 1–13.
8. Chen J, Wang Z, Zheng Z, et al. (2017) Neuron and microglia/macrophage-derived FGF10 activate neuronal FGFR2/PI3K/Akt signaling and inhibit microglia/macrophages TLR4/NF-kappaB-dependent neuroinflammation to improve functional recovery after spinal cord injury. *Cell Death Discov* 8: e3090.
9. Wynn TA, Barron L (2010) Macrophages: master regulators of inflammation and fibrosis. *Semin Liver Dis* 30: 245–257.
10. Liu HM, Wang DL, Liu CY (1990) Interactions between fibrin, collagen and endothelial cells in angiogenesis. *Adv Exp Med Biol* 281: 319–331.
11. Ismail N, Wang Y, Dakhlallah D, et al. (2013) Macrophage microvesicles induce macrophage differentiation and miR-223 transfer. *Blood* 121: 984–995.
12. Tricarico C, Clancy J, D'Souza-Schorey C (2017) Biology and biogenesis of shed microvesicles. *Small GTPases* 8: 220–232.
13. Obregon C, Rothen-Rutishauser B, Gerber P, et al. (2009) Active uptake of dendritic cell-derived exovesicles by epithelial cells induces the release of inflammatory mediators through a TNF-alpha-mediated pathway. *Am J Pathol* 175: 696–705.
14. Muralidharan-Chari V, Clancy J, Plou C, et al. (2009) ARF6-regulated shedding of tumor cell-derived plasma membrane microvesicles. *Curr Biol* 19: 1875–1885.
15. Wang T, Gilkes DM, Takano N, et al. (2014) Hypoxia-inducible factors and RAB22A mediate formation of microvesicles that stimulate breast cancer invasion and metastasis. *P Natl Acad Sci USA* 111: E3234– E 3242.

16. Martinez de Lizarrondo S, Roncal C, Calvayrac O, et al. (2012) Synergistic effect of thrombin and CD40 ligand on endothelial matrix metalloproteinase-10 expression and microparticle generation in vitro and in vivo. *Arterioscl Throm Vas* 32: 1477–1487.
17. Li CJ, Liu Y, Chen Y, et al. (2013) Novel proteolytic microvesicles released from human macrophages after exposure to tobacco smoke. *Am J Pathol* 182: 1552–1562.
18. Mochizuki S, Okada Y (2007) ADAMs in cancer cell proliferation and progression. *Cancer Sci* 98: 621–628.
19. Mezouar S, Darbousset R, Dignat-George F, et al. (2015) Inhibition of platelet activation prevents the P-selectin and integrin-dependent accumulation of cancer cell microparticles and reduces tumor growth and metastasis in vivo. *Int J Cancer* 136: 462–475.
20. Falati S, Liu Q, Gross P, et al. (2003) Accumulation of tissue factor into developing thrombi in vivo is dependent upon microparticle P-selectin glycoprotein ligand 1 and platelet P-selectin. *J Exp Med* 197: 1585–1598.
21. Del Conde I, Shrimpton CN, Thiagarajan P, et al. (2005) Tissue-factor-bearing microvesicles arise from lipid rafts and fuse with activated platelets to initiate coagulation. *Blood* 106: 1604–1611.
22. Pluskota E, Woody NM, Szpak D, et al. (2008) Expression, activation, and function of integrin $\alpha_M\beta_2$ (Mac-1) on neutrophil-derived microparticles. *Blood* 112: 2327–2335.
23. Garzetti L, Menon R, Finardi A, et al. (2014) Activated macrophages release microvesicles containing polarized M1 or M2 mRNAs. *J Leukocyte Biol* 95: 817–825.
24. Ward JR, West PW, Ariaans MP, et al. (2010) Temporal interleukin-1beta secretion from primary human peripheral blood monocytes by P2X7-independent and P2X7-dependent mechanisms. *J Biol Chem* 285: 23147–23158.
25. Zhang Y, Liu D, Chen X, et al. (2010) Secreted monocytic miR-150 enhances targeted endothelial cell migration. *Mol Cell* 39: 133–144.
26. Aras O, Shet A, Bach RR, et al. (2004) Induction of microparticle- and cell-associated intravascular tissue factor in human endotoxemia. *Blood* 103: 4545–4553.
27. Nguyen MA, Karunakaran D, Geoffrion M, et al. (2018) Extracellular vesicles secreted by atherogenic macrophages transfer microRNA to inhibit cell migration. *Arterioscl Throm Vas* 38: 49–63.
28. Soni S, Wilson MR, O'Dea KP, et al. (2016) Alveolar macrophage-derived microvesicles mediate acute lung injury. *Thorax* 71: 1020–1029.
29. Edgell CJ, McDonald CC, Graham JB (1983) Permanent cell line expressing human factor VIII-related antigen established by hybridization. *P Natl Acad Sci USA* 80: 3734–3737.
30. Thornhill MH, Li J, Haskard DO (1993) Leucocyte endothelial cell adhesion: a study comparing human umbilical vein endothelial cells and the endothelial cell line EA-hy-926. *Scand J Immunol* 38: 279–286.
31. Riesbeck K, Billstrom A, Tordsson J, et al. (1998) Endothelial cells expressing an inflammatory phenotype are lysed by superantigen-targeted cytotoxic T cells. *Clin Diagn Lab Immun* 5: 675–682.
32. Sokolov DI, Lvova TY, Okorokova LS, et al. (2017) Effect of cytokines on the formation tube-like structure by endothelial cells in the presence of trophoblast cells. *Bull Exp Biol Med* 163: 148–158.

33. van der Pol E, Coumans FA, Grootemaat AE, et al. (2014) Particle size distribution of exosomes and microvesicles determined by transmission electron microscopy, flow cytometry, nanoparticle tracking analysis, and resistive pulse sensing. *J Thromb Haemost* 12: 1182–1192.
34. Xu R, Greening DW, Zhu HJ, et al. (2016) Extracellular vesicle isolation and characterization: toward clinical application. *J Clin Invest* 126: 1152–1162.
35. Li P, Kaslan M, Lee SH, et al. (2017) Progress in Exosome Isolation Techniques. *Theranostics* 7: 789–804.
36. Simak J, Gelderman MP, Yu H, et al. (2006) Circulating endothelial microparticles in acute ischemic stroke: a link to severity, lesion volume and outcome. *J Thromb Haemost* 4: 1296–1302.
37. Sokolov DI, Ovchinnikova OM, Korenkov DA, et al. (2016) Influence of peripheral blood microparticles of pregnant women with preeclampsia on the phenotype of monocytes. *Transl Res* 170: 112–123.
38. Sokolov DI, Markova KL, Mikhailova VA, et al. (2019) Phenotypic and functional characteristics of microvesicles produced by natural killer cells. *Med Immunol (Russia)* 21: 669–688.
39. Korenevskii AV, Milyutina YP, Zhdanova AA, et al. (2018) Mass-Spectrometric Analysis of Proteome of Microvesicles Produced by NK-92 Natural Killer Cells. *B Exp Biol Med*+ 165: 564–571.
40. Evans-Osses I, Reichembach LH, Ramirez MI (2015) Exosomes or microvesicles? Two kinds of extracellular vesicles with different routes to modify protozoan-host cell interaction. *Parasitol Res* 114: 3567–3575.
41. Bradford MM (1976) A rapid and sensitive method for the quantitation of microgram quantities of protein utilizing the principle of protein-dye binding. *Anal Biochem* 72: 248–254.
42. Mikhailova VA, Belyakova KL, Vyazmina LP, et al. (2018) Evaluation of microvesicles formed by natural killer (Nk) cells using flow cytometry. *Med Immunol (Russia)* 20: 251–254.
43. Markova KL, Mikhailova VA, Korenevsky AV, et al. (2020) Microvesicles produced by natural killer cells of the NK-92 cell line affect the phenotype and functions of endothelial cells of the EA.Hy926 cell line. *Med Immunol (Russia)* 22: 249–268.
44. Sokolov DI, Furaeva KN, Stepanova OI, et al. (2015) Proliferative and migration activity of JEG-3 trophoblast cell line in the presence of cytokines. *B Exp Biol Med*+ 159: 550–556.
45. Markov AS, Markova KL, Sokolov DI, et al. (2019) Registration certificate No. 2019612366 for computer program “MarkMigration”. Available from: https://www.fips.ru/en/.
46. Gojova A, Barakat AI (2005) Vascular endothelial wound closure under shear stress: role of membrane fluidity and flow-sensitive ion channels. *J Appl Physiol* 98: 2355–2362.
47. Si Y, Chu H, Zhu W, et al. (2018) Concentration-dependent effects of rapamycin on proliferation, migration and apoptosis of endothelial cells in human venous malformation. *Exp Ther Med* 16: 4595–4601.
48. Markova KL, Kozyreva AR, Sokolov DI, et al. (2020) Microvesicles produced by natural killer cells regulate the formation of blood vessels. *B Exp Biol Med*+ 170: 123–127.
49. Ponce ML (2009) Tube formation: an in vitro matrigel angiogenesis assay. *Methods Mol Biol* 467: 183–188.

50. Waters WR, Harkins KR, Wannemuehler MJ (2002) Five-color flow cytometric analysis of swine lymphocytes for detection of proliferation, apoptosis, viability, and phenotype. *Cytometry* 48: 146–152.
51. Philpott NJ, Scopes J, Marsh JC, et al. (1995) Increased apoptosis in aplastic anemia bone marrow progenitor cells: possible pathophysiologic significance. *Exp Hematol* 23: 1642–1648.
52. Bass JJ, Wilkinson DJ, Rankin D, et al. (2017) An overview of technical considerations for Western blotting applications to physiological research. *Scand J Med Sci Spor* 27: 4–25.
53. Hamamura-Yasuno E, Aida T, Tsuchiya Y, et al. (2020) Immunostimulatory effects on THP-1 cells by peptide or protein pharmaceuticals associated with injection site reactions. *J Immunotoxicol* 17: 59–66.
54. Ito M, Yamamoto T, Watanabe M, et al. (1996) Detection of measles virus-induced apoptosis of human monocytic cell line (THP-1) by DNA fragmentation ELISA. *FEMS Immunol Med Mic* 15: 115–122.
55. Manna P, Jain SK (2014) Effect of PIP3 on adhesion molecules and adhesion of THP-1 monocytes to HUVEC treated with high glucose. *Cell Physiol Biochem* 33: 1197–1204.
56. Zhang X, Shang W, Yuan J, et al. (2016) Positive feedback cycle of TNFalpha promotes staphylococcal enterotoxin B-induced THP-1 cell apoptosis. *Front Cell Infect Microbiol* 6: 109.
57. Arjuman A, Chandra NC (2015) Differential pro-inflammatory responses of TNF-alpha receptors (TNFR1 and TNFR2) on LOX-1 signalling. *Mol Biol Rep* 42: 1039–1047.
58. Spiekermann K, Faber F, Voswinckel R, et al. (2002) The protein tyrosine kinase inhibitor SU5614 inhibits VEGF-induced endothelial cell sprouting and induces growth arrest and apoptosis by inhibition of c-kit in AML cells. *Exp Hematol* 30: 767–773.
59. Ligi D, Croce L, Mosti G, et al. (2017) Chronic venous insufficiency: transforming growth factor-β isoforms and soluble endoglin concentration in different states of wound healing. *Int J Mol Sci* 18: 2206.
60. Li X, O'Regan AW, Berman JS (2003) IFN-gamma induction of osteopontin expression in human monocytoid cells. *J Interf Cytok Res* 23: 259–265.
61. Liu JH, Wei S, Burnette PK, et al. (1999) Functional association of TGF-beta receptor II with cyclin B. *Oncogene* 18: 269–275.
62. Huang Y, Tian C, Li Q, et al. (2019) TET1 knockdown inhibits Porphyromonas gingivalis LPS/IFN-γ-induced M1 macrophage polarization through the NF-κB pathway in THP-1 cells. *Int J Mol Sci* 20: 2023.
63. Chen RF, Wang L, Cheng JT, et al. (2012) Induction of IFNalpha or IL-12 depends on differentiation of THP-1 cells in dengue infections without and with antibody enhancement. *BMC Infect Dis* 12: 340.
64. Barker KS, Liu T, Rogers PD (2005) Coculture of THP-1 human mononuclear cells with Candida albicans results in pronounced changes in host gene expression. *J Infect Dis* 192: 901–912.
65. Groh L, Keating ST, Joosten LAB, et al. (2018) Monocyte and macrophage immunometabolism in atherosclerosis. *Semin Immunopathol* 40: 203–214.
66. Chrobok NL, Sestito C, Wilhelmus MM, et al. (2017) Is monocyte- and macrophage-derived tissue transglutaminase involved in inflammatory processes? *Amino Acids* 49: 441–452.
67. Dalton HJ, Armaiz-Pena GN, Gonzalez-Villasana V, et al. (2014) Monocyte subpopulations in angiogenesis. *Cancer Res* 74: 1287–1293.

68. Laviv Y, Kasper B, Kasper EM (2018) Vascular hyperpermeability as a hallmark of phacomatoses: is the etiology angiogenesis related to or comparable with mechanisms seen in inflammatory pathways? Part II: angiogenesis- and inflammation-related molecular pathways, tumor-associated macrophages, and possible therapeutic implications: a comprehensive review. *Neurosurg Rev* 41: 931–944.
69. Andreu Z, Yanez-Mo M (2014) Tetraspanins in extracellular vesicle formation and function. *Front Immunol* 5: 442.
70. Colombo M, Raposo G, Thery C (2014) Biogenesis, secretion, and intercellular interactions of exosomes and other extracellular vesicles. *Annu Rev Cell Dev Bi* 30: 255–289.
71. Hemler ME (2003) Tetraspanin proteins mediate cellular penetration, invasion, and fusion events and define a novel type of membrane microdomain. *Annu Rev Cell Dev Bi* 19: 397–422.
72. Kalucka J, Bierhansl L, Wielockx B, et al. (2017) Interaction of endothelial cells with macrophages-linking molecular and metabolic signaling. *Pflug Arch Eur J Phy* 469: 473–483.
73. Levine SJ (2008) Molecular mechanisms of soluble cytokine receptor generation. *J Biol Chem* 283: 14177–14181.
74. Sedgwick AE, D'Souza-Schorey C (2018) The biology of extracellular microvesicles. *Traffic* 19: 319–327.
75. Mulcahy LA, Pink RC, Carter DR (2014) Routes and mechanisms of extracellular vesicle uptake. *J Extracell Vesicles* 3: 24641.
76. Rozmyslowicz T, Majka M, Kijowski J, et al. (2003) Platelet- and megakaryocyte-derived microparticles transfer CXCR4 receptor to CXCR4-null cells and make them susceptible to infection by X4-HIV. *AIDS* 17: 33–42.
77. Christianson HC, Svensson KJ, van Kuppevelt TH, et al. (2013) Cancer cell exosomes depend on cell-surface heparan sulfate proteoglycans for their internalization and functional activity. *P Natl Acad Sci USA* 110: 17380–17385.
78. Keskin U, Ulubay M, Dede M, et al. (2015) The relationship between the VEGF/sVEGFR-1 ratio and threatened abortion. *Arch Gynecol Obstet* 291: 557–561.
79. Guan XJ, Song L, Han FF, et al. (2013) Mesenchymal stem cells protect cigarette smoke-damaged lung and pulmonary function partly via VEGF-VEGF receptors. *J Cell Biochem* 114: 323–335.
80. Guerra A, Belinha J, Mangir N, et al. (2020) Sprouting angiogenesis: A numerical approach with experimental validation. *Ann Biomed Eng* 49: 871–884.
81. Hellbach N, Weise SC, Vezzali R, et al. (2014) Neural deletion of Tgfbr2 impairs angiogenesis through an altered secretome. *Hum Mol Genet* 23: 6177–6190.
82. Gallardo-Vara E, Tual-Chalot S, Botella LM, et al. (2018) Soluble endoglin regulates expression of angiogenesis-related proteins and induction of arteriovenous malformations in a mouse model of hereditary hemorrhagic telangiectasia. *Dis Models Mech* 11: dmm034397.
83. Pan CC, Bloodworth JC, Mythreye K, et al. (2012) Endoglin inhibits ERK-induced c-Myc and cyclin D1 expression to impede endothelial cell proliferation. *Biochem Bioph Res Co* 424: 620–623.
84. Roman AC, Carvajal-Gonzalez JM, Rico-Leo EM, et al. (2009) Dioxin receptor deficiency impairs angiogenesis by a mechanism involving VEGF-A depletion in the endothelium and transforming growth factor-beta overexpression in the stroma. *J Biol Chem* 284: 25135–25148.

85. Ling L, Maguire JJ, Davenport AP (2013) Endothelin-2, the forgotten isoform: emerging role in the cardiovascular system, ovarian development, immunology and cancer. *Brit J Pharmacol* 168: 283–295.
86. Lankhorst S, Danser AH, van den Meiracker AH (2016) Endothelin-1 and antiangiogenesis. *Am J Physiol-Reg I* 310: R230–R234.
87. Kandalaft LE, Motz GT, Busch J, et al. (2010) Angiogenesis and the tumor vasculature as antitumor immune modulators: the role of vascular endothelial growth factor and endothelin. *Cancer Immunol Immunother* 344: 129–148.
88. Sugimoto K, Yoshida S, Mashio Y, et al. (2014) Role of FGF10 on tumorigenesis by MS-K. *Genes Cells* 19: 112–125.
89. Walker DJ, Land SC (2018) Regulation of vascular signalling by nuclear Sprouty2 in fetal lung epithelial cells: Implications for co-ordinated airway and vascular branching in lung development. *Comp Biochem Phys B* 224: 105–114.
90. Hui Q, Jin Z, Li X, et al. (2018) FGF family: from drug development to clinical application. *Int J Mol Sci* 19: 1875.
91. Maretzky T, Evers A, Zhou W, et al. (2011) Migration of growth factor-stimulated epithelial and endothelial cells depends on EGFR transactivation by ADAM17. *Nat Commun* 2: 229.
92. Chen P, Zhang H, Zhang Q, et al. (2019) basic fibroblast growth factor reduces permeability and apoptosis of human brain microvascular endothelial cells in response to oxygen and glucose deprivation followed by reoxygenation via the fibroblast growth factor receptor 1 (FGFR1)/ERK pathway. *Med Sci Monit* 25: 7191–7201.
93. Winter SF, Acevedo VD, Gangula RD, et al. (2007) Conditional activation of FGFR1 in the prostate epithelium induces angiogenesis with concomitant differential regulation of Ang-1 and Ang-2. *Oncogene* 26: 4897–4907.
94. Parsons-Wingerter P, Elliott KE, Clark JI, et al. (2000) Fibroblast growth factor-2 selectively stimulates angiogenesis of small vessels in arterial tree. *Arterioscl Throm Vas* 20: 1250–1256.
95. Katoh M, Nakagama H (2014) FGF receptors: cancer biology and therapeutics. *Med Res Rev* 34: 280–300.
96. Siqueira M, Francis D, Gisbert D, et al. (2018) Radial glia cells control angiogenesis in the developing cerebral cortex through TGF-beta1 signaling. *Mol Neurobiol* 55: 3660–3675.
97. ten Dijke P, Arthur HM (2007) Extracellular control of TGFbeta signalling in vascular development and disease. *Nat Rev Mol Cell Bio* 8: 857–869.
98. Ding W, Shi W, Bellusci S, et al. (2007) Sprouty2 downregulation plays a pivotal role in mediating crosstalk between TGF-beta1 signaling and EGF as well as FGF receptor tyrosine kinase-ERK pathways in mesenchymal cells. *J Cell Physiol* 212: 796–806.

AIMS Press